University of Utrecht

European Severe Storms Laboratory

Master Thesis

Tornado Outbreaks in Europe

Author:
Lars Tijssen

Supervisors:
Pieter Groenemeijer
Aarnout van Delden

August 18, 2015

Contents

Abstract

Tornadoes in Europe have been documented and recorded in the European Severe Weather Database (ESWD) which is maintained by the European Severe Storms Laboratory (ESSL). The goal of this study is to find a useful definition of a tornado outbreak and to study the environmental differences between tornado outbreaks and individual tornadoes.

Tornado groups are created by an algorithm which dictates that if a tornado is located within a distance of 500 km spatially and 6 hours temporally of another tornado, then these tornadoes belong to the same group. From these groups the groups which have a cumulative Fujita scale number of 7 or higher are given the tornado outbreak status. This way the tornado groups which have a high number of tornadoes or several strong tornadoes are retained.

Two reanalysis datasets are used in this study. The ERA-Interim reanalysis dataset provided by the ECMWF and the Climate Forecast System Reanalysis (CFSR) dataset provided by NCAR. Both datasets cover the 1979 - 2014 period. Several convective parameters are computed from these datasets which include mixed layer CAPE (MLCAPE), mixed layer lifting condensation level (MLLCL), deep layer shear (DLS), low level shear (LLS) and both 0-3 km and 0-1 km storm relative helicity (SRH).

By taking a local maximum (minimum for LCL) of each convective parameter in a local spatial and temporal domain, each tornado in the ESWD in the 1979 - 2014 period is assigned a value for each of the convective parameters. It is found that tornadoes inside outbreaks are associated with higher values of DLS, LLS and to a lesser extent SRH and MLCAPE compared to tornadoes outside outbreaks. In tornado environments significant differences exist between the reanalysis datasets. In the large majority of tornado occurrences the CFSR convective parameters have higher values than their ERA-Interim counterparts.

1 Introduction

1.1 History of Tornado Research

Tornadoes have long since been reported in various places in the world. Stories about tornadoes go back to the beginning of time. The first written reports of tornado events start in the first millennium. Often these records come from stories and poems that are written by scribes or monks which is the only source of information that is available for these events. Knowledge of tornadoes around those times was practically non-existent and therefore tornadoes and encounters with them were often attributed to gods, devils or other folklore. Tornadoes were most often documented when they occur near to towns/cities where people could observe them or left behind visible destruction. An example of such an event is shown in figure 1 where a tornado has destroyed the nave of the dom church in Utrecht, The Netherlands. The destruction of the church was so big that it was decided not to rebuild the church. Therefore only the tower remains to this day.

Figure 1: A tornado caused the collapse of the nave of the dom church of Utrecht in 1674. The nave was never rebuild and only the tower remains to this day. Source: Het Utrechts Archief: Drawings by Herman Saftleven.

Until the start of the twentieth century research on tornadoes had not gotten very far. In 1917 the famous geophysicist, meteorologist and polar researcher Alfred Wegener, who is best known for his revolutionary ideas on continental drift, wrote a book called *Wind- und Wasserhosen in Europa* (Wegener (1917)).

He was the first to discuss tornado occurrences on a European level in this book. He also noted that there should be at least 100 yearly occurrences of tornadoes throughout Europe. This has been proven to be correct (Groenemeijer and Kühne (2014)).

Modern day research into tornadoes started in the early fifties in the USA but really took flight when Ted Fujita of the University of Chicago started to research tornadoes in the sixties and seventies (Bluestein (1999)). Fujita studied tornado damage intensively during his career and introduced the Fujita-scale, where tornadoes are categorized into five separate levels according to the from damage estimated wind speed (Fujita et al. (1971)). He also concluded after researching tornado damage that tornadoes can consist of sub vortices and identified non-tornadic meteorological phenomena such as downbursts and microbursts. One of the inventions that really helped with tornado research was the invention of weather radar, on which the structure of thunderstorms could be made visible. Researchers in the early fifties found that some storms exhibited a small hole where the radar reflection was very low. This resulted in a storm displaying a "hook" on the radar image. This display phenomenon was coined a "hook echo" due to its hook like shape. Around the same time it was noticed that these hook echoes and tornadoes were correlated.

Research in Europe started quite a bit later than in the USA. In 1997 a first attempt was made to build a climatology of tornadoes and other severe weather phenomena of the countries Germany, Austria and Switzerland by the Tor-DACH network. This database of severe weather was used to make estimates of tornado occurrence in these countries (Dotzek (2001)). In 2002 the TorDACH network was succeeded by the founding of the European Severe Storms Laboratory (ESSL) network and the European Severe Weather Database (ESWD) which incorporated the previous TorDACH data and other datasets in an effort to create a pan-European severe weather database. Both the TorDACH network and the ESSL were spearheaded by Nikolai Dotzek who both put in a lot of effort in creating these networks and doing research using these to build a climatology of tornadoes in Europe (Dotzek (2003), Bissolli et al. (2007)). After his early death in 2010 the ESSL appointed Pieter Groenemeijer as the new director. Under his supervision the ESSL grew to what it is today: A non-profit research organization with multiple researchers who work part- or full-time researching tornadoes and other severe weather phenomena in Europe. The latest findings on tornado climatology in Europe from the ESWD are presented in Groenemeijer and Kühne (2014).

1.2   Research Goals

The main focus of this study will be tornadoes in the ESWD and reanalysis datasets. This study will try to answer the following questions:

- Is it possible to create a workable definition of a tornado outbreak in Europe?

4

- How can the environments of European tornado outbreaks be characterized?

- Do European tornado outbreak environments differ from European single tornado environments?

- Is there a difference in European tornado outbreak environments between different reanalysis datasets?

- What are the differences in European tornado outbreak environments between summertime and wintertime?

1.3 Overview

In the next section some detailed explanation will be given pertaining the data used in this study. In this section both the tornado data from the ESWD and the fields from the reanalysis datasets will be discussed as well as the convective parameters that are calculated from these fields. In the Methods section both the coupling between tornado reports and definition of a tornado outbreak will be discussed. In the Results section both the found tornado outbreaks and the results of the convective parameter coupling will be discussed. Finally a Conclusion and Discussion are written where respectively the results from the study will be concluded and limitations of the study will be discussed.

2 Data

2.1 European Severe Weather Database and tornado data

The European Severe Weather Database is a database containing severe weather reports from all over Europe. Users are encouraged to report as many details as possible about weather phenomena they encounter. Phenomena that are reported include wind damage (straight line wind damage or tornado damage), hail over 2 centimeters, high rain rates or flash flood damage and tornado sightings. These reports are accompanied by a time stamp, longitude/latitude details and often also include images or videos of the event. Extra information pertaining the details of the event can also be added. Reports get a quality check ranging from QC0 (where an event is unverified) to QC2 (where an event is fully verified by an expert in the field). At this moment there are more than 80000 severe weather reports (large hail, severe wind, heavy rain and tornado reports. Excluding QC0) of which more than 6500 are tornado reports. These reports also include land- and waterspouts. Most tornadoes have a strength rating according to the aforementioned F (Fujita) scale which ranges from F0 (very weak) to F5 (very strong). There are also reports of tornadoes with an unknown F scale rating. These tornadoes consist mainly of F0 tornadoes (Grünwald and Brooks (2011), Groenemeijer and Kühne (2014)) and are therefore included in the F0 tornado category for the purpose of this study.

2.2 Reanalysis Data

Reanalysis datasets are playing an ever increasing role in modern meteorology research. They are an attempt to reconstruct the state of the atmosphere by incorporating various atmospheric observations. Many different surface and upper air observations are used to construct an analyses state. This analyzed state is then used by an operational model to forecast for number of periods in the future. In this study only the analyzed state will be used.

Two different reanalysis datasets will be used in this research: The ERA-Interim reanalysis and the CFSR reanalysis. Of these reanalyses datasets, a number of fields will be used to calculate convective parameters. These convective parameters will then be assigned to tornadoes from the ESWD in section 2.3.

2.2.1 ERA-Interim

The ERA-Interim reanalysis is the latest global atmospheric reanalysis produced by the European Centre for Medium range Weather Forecasts (ECMWF) (Dee et al. (2011)). It is the successor to the successful ERA-40C reanalysis. It currently covers the period 1 Jan 1979 to 31 Dec 2014 while regularly being updated. The core numerical model is a 2006 release of the numerical weather model IFS which is also operated by the ECMWF. It has a T255 spectral resolution which outputs on a grid with grid spacing $0.75°$ and 60 vertical models. Surface fields are available every 3 hours, whereas upper level fields are available every 6 hours.

2.2.2 CFSR

The Climate Forecast System Reanalysis (CFSR) is the second reanalysis dataset that is used in this study. It is a product of the National Centers for Environmental Prediction (NCEP). This reanalysis has a T382 horizontal spectral resolution and 64 vertical levels which outputs on a horizontal grid with grid spacing $0.5°$ (Saha et al. (2010)). The core numerical model is the newly developed fully coupled atmospheric-ocean-land model CFSv2 which is also used by the NCEP to make daily and monthly/seasonal weather predictions (Saha et al. (2014)). It currently covers the period 1 Jan 1979 to 31 Aug 2014 while regularly being updated. Both surface fields and upper level fields are available every 6 hours. A summary of the properties of each reanalysis can be found in table 1.

Of both reanalysis datasets the upper level data for the following 5 variable fields are retrieved: temperature, water vapor mixing ratio, geopotential, u-component wind and v-component wind. These variables are extracted from 28 different pressure levels between 1000hPa and 70hPa on a horizontal domain that covers Europe fully. The surface fields that are retrieved are: Surface geopotential and surface pressure. All fields are retrieved for the entire available period of the reanalysis (ERA-Interim: 1 Jan 1979 - 31 Dec 2014, CFSR: 1 Jan 1979 - 31 Aug 2014).

Reanalysis Name	ERA-Interim	CFSR
Core Numerical Model	IFS (2006)	CFSv2
Period	1979 - 2014	1979 - Aug 2014
Resolution (spectral)	T255	T382
Resolution (projected)	0.75°	0.5°
Vertical levels	60	64

Table 1: Properties of reanalysis datasets.

2.3 Convective Parameters

From the variable fields retrieved the following special variables are calculated

2.3.1 Mixed Layer CAPE

Convective Available Potential Energy (CAPE) is a variable that is frequently used to forecast convective storms. Like the name suggests it describes the amount of energy that a storm can use in its ascending phase. It also denotes the theoretical maximum updraft speed of the parcel in absence of entrainment and drag forces. Generally speaking, the higher the CAPE value, the more vigorous the updraft which also increases the risk of severe weather. It is calculated as the integral between the parcel temperature profile and the environment temperature profile, where the parcel temperature is higher than the environment temperature. The lower boundary of the integral is called the Level of Free Convection (LFC), whereas the upper boundary is called the Equilibrium Level (EL). In mathematical form:

$$CAPE = g \int_{z_{LFC}}^{z_{EL}} \frac{Tv,parcel - Tv,env}{Tv,env} dz \qquad (1)$$

Where g is the gravitational acceleration, z_{LFC} is the height of the LFC, z_{EL} is the height of the EL, $Tv,parcel$ is the virtual temperature of the ascending air parcel and Tv,env is the virtual temperature of the environment. This formula can also be written in pressure coordinates:

$$CAPE = -R_d \int_{p_{LFC}}^{p_{EL}} (Tv,parcel - Tv,env) dlnp \qquad (2)$$

where R_d is the gas constant for dry air, p is the pressure, p_{LFC} is the pressure at the LFC and p_{EL} is the pressure at the EL. The aforementioned theoretical maximum updraft speed is given by:

$$w_{max} = \sqrt{2 * CAPE} \qquad (3)$$

CAPE can be calculated in various ways, depending on the initial temperature, humidity and pressure of the lifted parcel. There is Surfaced Based CAPE (SBCAPE) which, as the name suggests, starts with an ascending parcel near the surface. This method of calculating CAPE can vary strongly in time and space and can overestimate updraft speeds in the case of a very thin and not

well mixed surface layer with high temperature and humidity (Bunkers et al. (2002)). Therefore SBCAPE might not be the best choice for the purpose of this study. Alternatively one can calculate the Mixed Layer CAPE (MLCAPE) where instead of a parcel with surface values one calculates an average value over a certain depth of the surface layer. Typical values that are taken for the extent of the mixed layer above the surface are for example: 30hPa, 50hPa or 100hPa. To include as many data points and to minimize surface influence a depth of 100hPa for the mixed layer is used. This includes up to 3 data pressure levels (interval between pressure levels in the lower layers of the atmosphere is 25hPa). The surface value is not taken directly from the model but rather calculated from the lowest pressure level assuming a well mixed layer. This means that surface temperature is estimated from a dry adiabatic profile and surface mixing ratio is equal to that of the lowest pressure level above the surface. This assumption means that MLCAPE might be overestimated during the late evening, night and morning hours when a nighttime inversion has replaced a well mixed layer. However since the depth of the layer is set to 100hPa this deviation might be small. The value at 100hPa above the surface is calculated using linear interpolation between pressure points. Therefore the mixed layer values are calculated by making a weighted average over the aforementioned points. These values are then used to calculate the MLCAPE.

2.3.2 Mixed Layer Lifting Condensation Level

The lifting Condensation Level (LCL) is the height above the layer at which a parcel ascending from that layer will start to condensate and cloud formation will start to take place. It is calculated from the following formula (Bolton (1980)):

$$T_{LCL} = \frac{2840}{3.5 * ln(T) - ln(e) - 4.805} + 55 \tag{4}$$

Where T_{LCL} is the temperature of the lifting condensation level, T is the temperature and e is the vapor pressure of the surface. When calculating the mixed layer LCL, the surface values for T and e are replaced by those of the mixed layer.

2.3.3 Deep Layer Shear and Low Level Shear

Deep Layer Shear (DLS), also known as the bulk shear, is a variable that describes storm organization. It is calculated by subtracting the 10m horizontal wind field from the horizontal wind field 6 km above the surface:

$$\vec{u}_{DLS} = \vec{u}_{6km} - \vec{u}_{10m} \tag{5}$$

Where $\vec{u}_{DLS}$ is the deep layer shear wind vector, $\vec{u}_{6km}$ is the horizontal wind vector 6 km above the surface and $\vec{u}_{10m}$ is the horizontal wind vector 10m above the surface.

The values of the wind 10m above the surface are acquired by linearly interpolating the wind at pressure levels to the surface. This is less accurate than directly taking the 10m horizontal wind field output from the model, but was necessary because CFSR surface fields were not available at the same resolution

as the upper level fields so that they could not be used. The values of the wind 6 km above the surface are calculated by linear interpolation between the two nearest pressure levels. Low DLS indicate that storms are weakly organized which limits their severe weather potential. High values indicate that storms can become organized into systems larger than an individual storm cell (Weisman and Klemp (1982)). The severe weather potential with organized storms is usually higher than with weakly organized storms. Supercells which are associated with tornadoes generally favor high deep layer shear values.

Like deep layer shear, low level shear is a vector denoting the horizontal wind difference between two layers. It is calculated by subtracting the surface horizontal wind field from the horizontal wind field 1 km above the surface. The values of the wind 1 km above the surface are calculated by linear interpolation between the two nearest pressure levels. High values of LLS indicate that wind increases strongly with height near the surface. This can augment the risk of tornadoes (Davies and Johns (1993)).

2.3.4   Storm Relative Helicity

Storm Relative Helicity (SRH) is a measurement of how much low level 'rotation' is ingested by the storm. This is a very important variable for supercell storms and therefore for tornado formation. To calculate the storm relative helicity one first has to calculate the storm motion. This storm motion indicates the direction possible supercells are moving. To calculate the storm motion take the mean wind in the 0-6 km layer and add a deviation based on the 0-6 km deep layer wind shear:

$$\vec{c} = \vec{V}_{mean} + 7.5 \left[\frac{\vec{V}_{DLS} \times \hat{k}}{|\vec{V}_{DLS}|} \right] \tag{6}$$

where $\vec{c}$ is the storm motion vector, $\vec{V}_{mean}$ is the mean wind vector, $\vec{V}_{DLS}$ is the deep layer shear vector and $\hat{k}$ is the vertical unity vector (Bunkers et al. (2000)). This variable is used to calculate the storm relative helicity:

$$SRH = \int_0^d (\vec{V} - \vec{c}) \cdot \vec{\omega}_h dz \tag{7}$$

Which is the integrated value of the dot product between the storm relative horizontal wind field $(\vec{V} - \vec{c})$ and the horizontal vorticity $\vec{\omega}_h$ between the surface and a certain height d. Two variations of storm relative helicity are used in this study: The storm relative helicity 0-3 km (where $d = 3$ km) and the storm relative helicity 0-1 km (where $d = 1$ km).

3 Methods

3.1 Coupling Tornadoes and Reanalysis Data

Now that the convective parameters have been calculated, it is important to think on how to assign said parameters to tornado outbreaks. Ideally, tornadoes would occur at positions in time and space where reanalysis data is available but, unfortunately, for almost all tornadoes this is not the case. Therefore a technique is needed to assign a realistic reanalysis value to a tornado where no reanalysis data is available. One technique can be to simply linearly interpolate data in space and time (so in three dimensions: time, latitude, longitude). This seems like a feasible idea, however this technique has a big downside. Especially in cases where, for example, fast fluctuating parameters are quickly moving through the area of interest. Since reanalysis data is only available every 6 hours, it is possible that at 12Z a cape maximum lies west of the tornado while at 18Z the cape maximum has traversed to an area east of the tornado. In case the tornado occurred at 15Z, it is very likely that this tornado is associated with the CAPE maximum. But using linear interpolation, one will never see this maximum assigned to the tornado since the interpolation is based on information at the tornado location at times 12Z and 18Z. This situation is illustrated in figure 2. Therefore a technique must be developed that will assign a more representative CAPE to the tornado.

A second technique is to take the maximum value in the area around the tornado out of the two nearest reanalysis times. This is shown in figure 2 by the two bottom images, where a $3° \times 3°$ blue square has been drawn around the tornado. The choice for a square $3° \times 3°$ is made out of simplicity due to the overlap of boundaries of the reanalysis datasets (ERA $0.75°$ and CFSR $0.5°$). This yields much more accurate results compared to linear interpolation and will therefore be used in this study to assign every tornado a convective parameters. The exception is the mixed layer LCL for which lower values are usually associated with severe weather. Therefore, instead of a maximum a minimum will be sought for mixed layer LCL.

Using the maximum value technique, every tornado in the ESWD that happened between 1 Jan 1979 and 31 Aug 2014 has been assigned a convective parameter value.
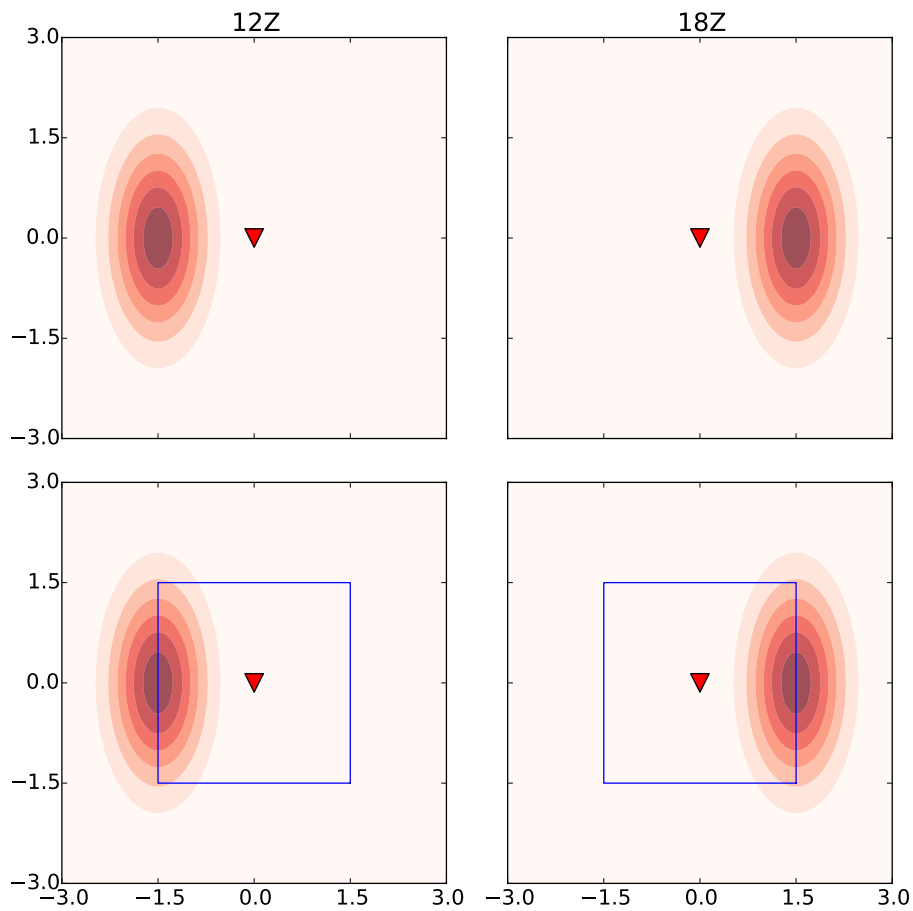
Figure 2: A theoretical example of a fast moving field. The field is indicated by the red colored area with the highest values indicated by the dark spot. The tornado is indicated by the red triangle in the center. The numbers on the axes indicate degrees with respect to the tornado. There is a time difference of 6 hours between the images on the left and the images on the right. The upper images demonstrate that when taking values from both times at the location of the tornado the result is going to be zero. The lower images demonstrate that, when taking the maximum value from within the 3° x 3° blue square, the tornado will be associated with the field's maximum.

3.2   Tornado Outbreak Definition

Sometimes storm systems can produce one or more tornadoes if environmental conditions are right. If the tornadoes are severe enough or a large number of tornadoes form this might be called a *Tornado Outbreak*. However, the definition of tornado outbreak varies a lot. Even in the USA, where most of the tornado research has taken place, a solid definition for a tornado outbreak is lacking. Pautz (1969) suggested a number dependent definition where a small outbreak would be 6-10 tornadoes, moderate would be 11-20 tornadoes and large would be more than 20 tornadoes. Galway (1977) defined an outbreak as 10 or more tornadoes. Doswell III et al. (2006) base their definition on a complex number of factors including but not limited to: the number of tornadoes, the number of violent (F4 and F5) tornadoes, the path length of each tornado, the number of fatalities and the number of tornadoes with track length $\geq$ 80 km. This is a very advanced way of making a definition, depends on the local tornado climatology and is therefore very location specific. Thus, a definition like this for the USA will not work for Europe.

Due to these inconsistent definitions and the fact that the definitions are regionally dependent, it is vital that for this study a new definition is introduced that will work for European tornado occurrence and with the reports that are recorded in the ESWD thus far. All tornado definitions mentioned previously agree that days where an unusually large amount of tornadoes happen (for example the super outbreak of 1974 or 3 May 1999 in the USA) should definitely be defined as an outbreak. But a single tornado should, for obvious reasons, not be included in an outbreak definition. Somewhere between these two extremes the line should be drawn to decide what is an outbreak and what is not.

Since the previously mentioned definitions agree that a large amount of tornadoes must happen within close temporal and spatial distance from each other, the most obvious approach towards forming a tornado definition would be based on these variables. Therefore, a method has been developed in this study to define a tornado outbreak based on the distance r and time t between successive tornadoes. Tornado reports from the ESWD will serve as the foundation for this method. The method consists of two parts. In part one all tornadoes are assigned a number. Two tornadoes that are within a distance r and time t of each other are assigned the same number. This step is visualized in figure 3. In this way sequences of tornadoes with the same number are created which will hereafter be referred to as *tornado groups* or simply *groups*.

The first step of the tornado outbreak detection method is applied to tornado reports between 1 Jan 1900 and 31 Aug 2014. In figure 4, a number of statistics are displayed about the formed tornado groups as a function of distance r and time t. Six values for both r and t are chosen: 6, 12, 18, 24, 30 and 36 hours for t and 100, 200, 500, 1000 and 2000 km for r. The total number of groups decreases as r and t increase. This can be explained because with larger values of these variables tornado groups get joined together. This is also visible in the average number of tornadoes per group, which increases as r and t get bigger. The fraction of groups containing one tornado decreases with increasing r and t as groups get bigger, but is still quite big. This means that quite a large
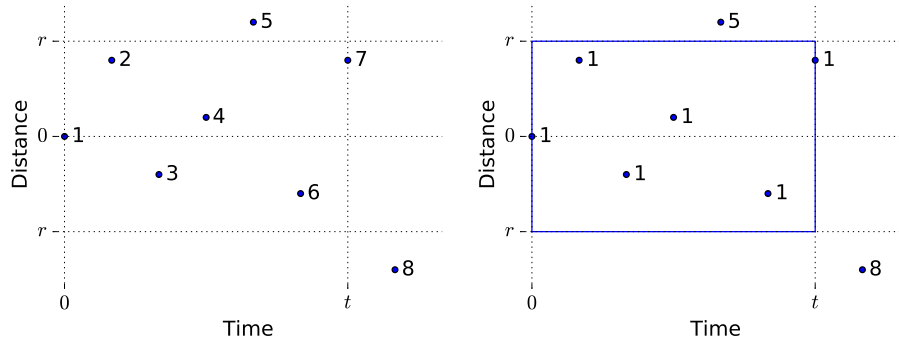
Figure 3: Two figures displaying an example of how step one of the outbreak method works. Eight dots are displayed which resemble tornado reports from the ESWD. The tornado with number one is the reference tornado to which all other tornadoes are compared. On the vertical and horizontal axes the distance and time are displayed respectively, with the reference tornado at point (0,0). All tornadoes within time t and distance r of the reference tornado are then assigned the same number as the reference tornado, which is displayed in the figure on the right. Tornado number five and eight do not meet the requirements and therefore keep their original number. The method then moves on the the next tornado report (tornado number 2 in the left figure) and repeats the process.
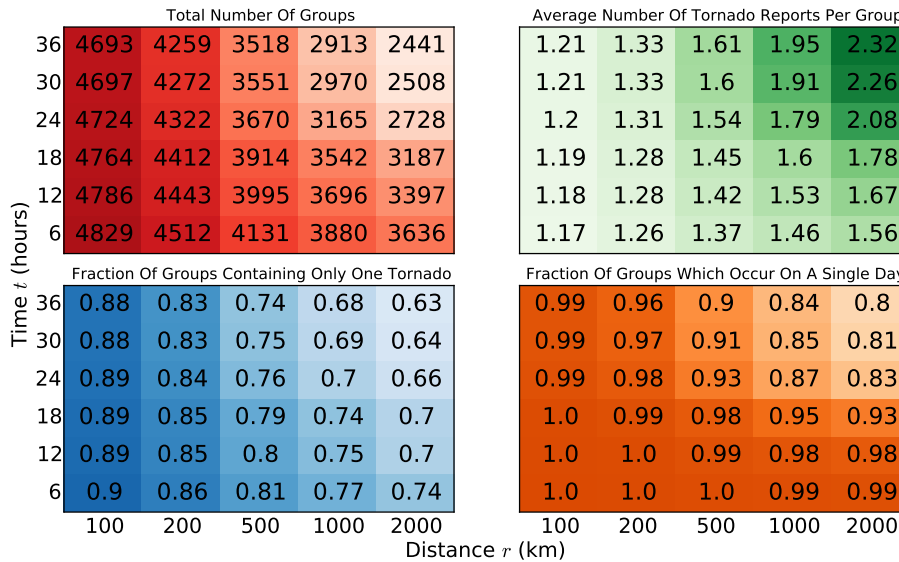

Figure 4: Statistics of tornado groups as a function of r and t for ESWD tornado reports between 1 Jan 1900 and 31 Aug 2014. Upper left: Total number of tornado groups. Upper right: The average number of tornado reports per group. Lower left: The fraction of groups containing only one tornado report. Lower right: The fraction of groups which total duration is 24 hours or less.

14

number of tornadoes in the database occur solitary or at least far away from other tornadoes in both space and time. The last table in the bottom right corner displays the fraction of groups which have a total duration of 24 hours or less. Take note that this also includes the groups that comprise of only one tornado which automatically meet this requirement. It can be seen that the fraction is or is close to 1 for low r and t. However this ratio decreases as r and t increase, which means more and more groups are spread over multiple days. The transition seems to be greatest between 18 and 24 hour values for t when r is large. This suggest that between these two t values a large transition occurs from groups limited to one day to groups spreading over two or more days. This is very likely caused by the daily cycle in thunderstorm activity.

The second step is to make a sub selection of the groups by some severity criteria. There are multiple ways to do this. One can simply select based on a minimum number of tornadoes per group (Pautz (1969), Galway (1977)). This will exclude small groups but retain larger ones. However this also means that small groups of strong tornadoes are also excluded. Another way of selecting is to retain groups which have at least one significant tornado (F2 or stronger). This will include small groups of strong tornadoes too. However this includes groups with only one tornado and excludes large groups with only weak tornadoes which might also be of interest. A third option exists which combines the previous two options: One can demand that the sum of the F scale of all the tornadoes in a group meets a certain minimum. This allows one to retain both small groups with a few strong tornadoes as well as large groups which contain comparable less strong tornadoes. The tornado groups that meet this requirement are then upgraded to *Tornado Outbreak* or simply *Outbreak* status. However, one needs to be careful in deciding that threshold value to take. Take a value that is too low and very small groups of one or two tornadoes are also included. Take a value that is too large and one might end up with only a few or no groups that meet the requirement. From multiple experiments it is determined that a threshold value of 7 is a decent compromise. In figure 5, a number of statistics have been compiled for outbreaks with the threshold F scale sum value is set to 7. In the table in the upper left one can see that the total number of tornadoes in all outbreaks increases with both r and t. This can be seen from the other tables, as both the number of outbreaks and average number of tornadoes per outbreak increases. The number of outbreaks for small r and t is still quite high (20-30 outbreaks). The reason for that is the relatively low F scale threshold value. The total number and average number of tornadoes are also quite large for small r and t values. This is caused by one very big outbreak (UK 1981) which will be discussed in the next section. The last table denotes the fraction of outbreaks with a duration of 24 hours or less.

Based on these statistics, a choice must be made for which value of r and t to use. This choice is not straightforward, as the reason for choosing certain values can all be viable reasons. For example, one can choose a high value for r and t if one wants to include multi day outbreaks. This can also be a good reason if one wants to increase the number of tornado outbreaks. Oppositely one can choose small values for r and t if one wants to study a small number of outbreaks and/or one day outbreaks. Since in this study reanalysis data has to be coupled to tornadoes it is an advantage to have short lasting tornado out-
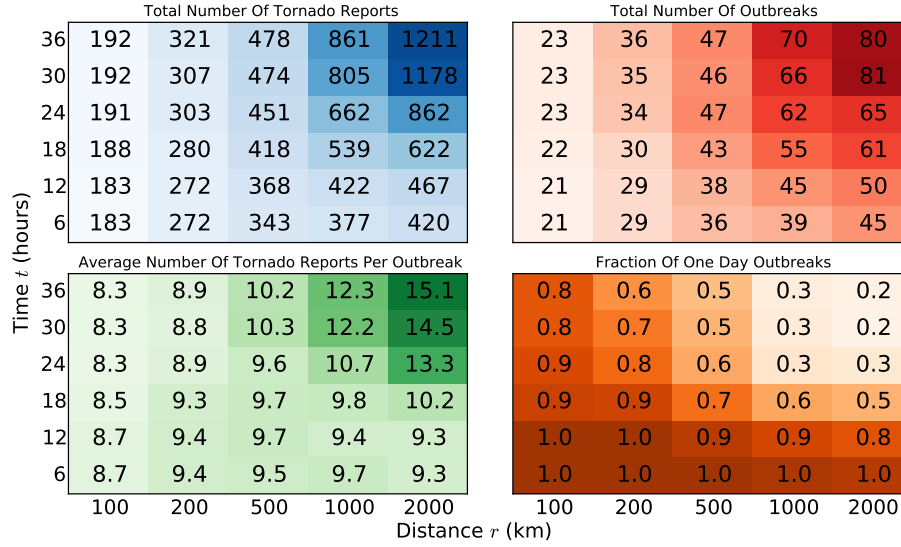
Figure 5: Statistics of tornado outbreaks as a function of r and t for ESWD tornado reports between 1 Jan 1900 and 31 Aug 2014. The threshold F scale sum value is set to 7. Upper left: Total number of tornado reports in all outbreaks. Upper right: The total number of outbreaks. Lower left: The average number of tornado reports per outbreak. Lower right: The fraction of outbreaks which total duration is 24 hours or less.

Variable	Threshold
Distance r	500 km
Time t	6 hours
F scale sum	7

Table 2: A summary of the values taken for r, t and F scale sum.

breaks. Therefore in this study the value for t will be 6 hours. The value of r shall be with 500 km an intermediate value to still retain a significant amount of tornado outbreaks. From figure 5 it can be seen that 36 outbreaks are left. These outbreaks will be presented in the next section.

4 Results

In this section the results of the tornado outbreak method will be presented. In total there are 36 tornado outbreaks between 1 Jan 1900 and 31 Aug 2014 detected. First a number of statistics will be presented about these tornado outbreaks. A highlight with a short description about some of the more notable outbreaks will be given as well. After that, tornado outbreaks (and individual tornadoes will be compared with reanalysis data. Lastly, some comments will be made on the differences between reanalysis data.

4.1 Tornado Outbreaks

There are 36 tornado outbreaks detected in the ESWD period that was selected with the given r and t in table 2. In table 3 all outbreaks are listed in chronological order. In addition to the outbreak number, date and countries the tornadoes occurred a number of interesting statistic has been added in this table. Since the sum of the F scale numbers in the outbreaks must be 7 or larger, this is the lowest number we find in the F sum column. In figure 6 all tornado outbreaks have been displayed geographically. Each tornado outbreak in this figure is represented by its geographical center.
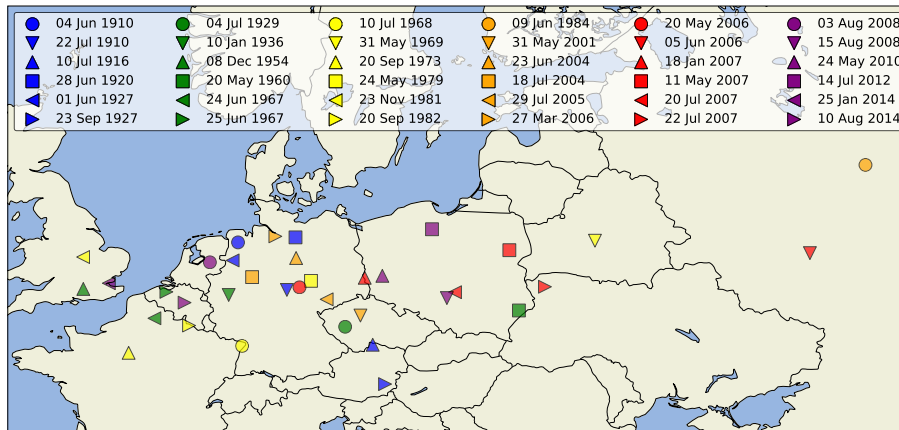

Figure 6: A figure of all 36 European tornado outbreaks in the period 1 Jan 1900 to 31 Aug 2014. Plotted is the geographical center of each outbreak. The legend indicates the day the outbreak began.

The outbreaks that are detected are broadly in an area from the UK over central Europe into Russia. No tornado outbreaks are detected in Southern Europe nor in Northern Europe. This is not surprising considering that the ESWD suffers from under reporting in these areas because of low population density (Northern Europe, the Alps and North Africa), datasets which have not been integrated into the ESWD (Spain, Greece, Turkey) or little contact with local tornado researchers (some of the Balkan countries, North Africa, Middle East) (Groenemeijer and Kühne (2014)). Tornado reports in the ESWD have a very

	Date	Countries	Tor num	F sum	F max	F mean
OUTBREAK						
1	04 Jun 1910	[DE]	2	7	4	3.5
2	22 Jul 1910	[DE]	11	7	3	0.6
3	10 Jul 1916	[DE, AT]	3	9	4	3
4	28 Jun 1920	[DE]	7	14	3	2
5	01 Jun 1927	[DE, BE]	5	10	4	2
6	23 Sep 1927	[AT]	3	7	3	2.3
7	04 Jul 1929	[CZ, DE]	8	14	3	1.8
8	10 Jan 1936	[DE]	2	7	4	3.5
9	08 Dec 1954	[UK]	7	7	3	1
10	20 May 1960	[PL, UA]	8	12	4	1.5
11	24 Jun 1967	[FR]	3	12	5	4
12	25 Jun 1967	[FR, BE, NL]	5	13	3	2.6
13	10 Jul 1968	[FR, DE]	2	7	4	3.5
14	31 May 1969	[BY]	4	7	2	1.8
15	20 Sep 1973	[FR]	3	9	3	3
16	24 May 1979	[DE]	6	9	4	1.5
17	23 Nov 1981	[UK]	104	74	2	0.7
18	20 Sep 1982	[FR, BE]	3	8	3	2.7
19	09 Jun 1984	[RU]	17	13	5	0.8
20	31 May 2001	[CZ, DE]	6	7	2	1.2
21	23 Jun 2004	[DE]	5	9	3	1.8
22	18 Jul 2004	[DE]	3	7	3	2.3
23	29 Jul 2005	[DE, CZ]	8	13	2	1.6
24	27 Mar 2006	[DE]	8	9	2	1.1
25	20 May 2006	[DE, CZ, PL]	15	17	2	1.1
26	05 Jun 2006	[RU]	14	9	2	0.6
27	18 Jan 2007	[DE, PL, CZ]	8	18	3	2.2
28	11 May 2007	[PL, BY, UA]	13	11	2	0.8
29	20 Jul 2007	[PL]	4	7	3	1.8
30	22 Jul 2007	[UA, PL]	8	14	3	1.8
31	03 Aug 2008	[NL, DE, FR]	4	9	4	2.2
32	15 Aug 2008	[PL]	10	16	3	1.6
33	24 May 2010	[DE, PL]	7	10	3	1.4
34	14 Jul 2012	[PL]	3	7	3	2.3
35	25 Jan 2014	[UK, FR, BE]	12	12	2	1
36	10 Aug 2014	[FR, UK, NL, BE, DE]	12	11	2	0.9

Table 3: A list of all tornado outbreaks sorted chronologically. from left to right: Outbreak number, date, the countries where the tornadoes occurred, the sum of the F scale of the tornadoes within the outbreak, the number of tornadoes, the strongest tornado strength within the outbreak and the mean F scale number of all tornadoes.

high density across Germany, the Netherlands, Belgium, France, Austria, the Czech Republic and Poland which correspond to areas where most outbreaks have been detected. The temporal distribution of the outbreaks is also quite interesting. Over half of the outbreaks have occurred in the twenty-first century which only comprises twelve percent of the total period length. This is consistent with the fact that the number of tornado reports has increased dramatically since the turn of the century (Groenemeijer and Kühne (2014)).
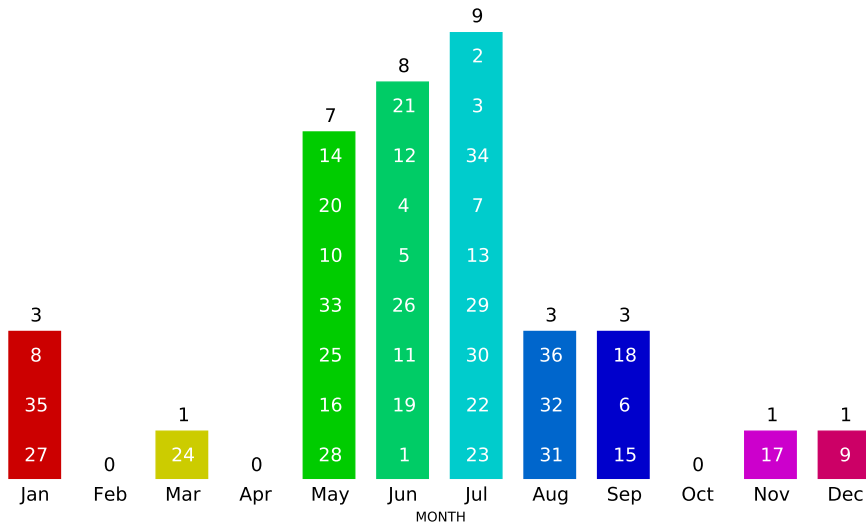
Figure 7: All 36 European tornado outbreaks listed by month of occurrence. The number in the column refers to the outbreak number named in table 3. The number above the column refers to the total number of outbreaks in this month.

In figure 7 all tornado outbreaks are sorted by their respective month. Most outbreaks took place in the months May, June and July. A number of tornado outbreaks have happened in the months August, September and January. The months March, November and December all have one outbreak. This distribution matches the distribution of tornadoes in the ESWD for the months May, June and July but for the number of tornadoes August seems to have few outbreaks as is visible from 8. It should be noted that 36 is still quite a low number for statistics. Therefore reliable statements can not be made.

in the next sections a number of notable and previously studied European tornado outbreaks will be discussed.

4.1.1 Outbreak 11 and 12: 24 and 25 June 1967

These two tornado outbreaks happened on two consecutive days, making for a rather extraordinary double outbreak. This outbreak features one of the two F5 tornadoes in the tornado outbreaks, the other one occurring near Ivanovo, Russia in 1984. Records on damage from these outbreaks are numerous but
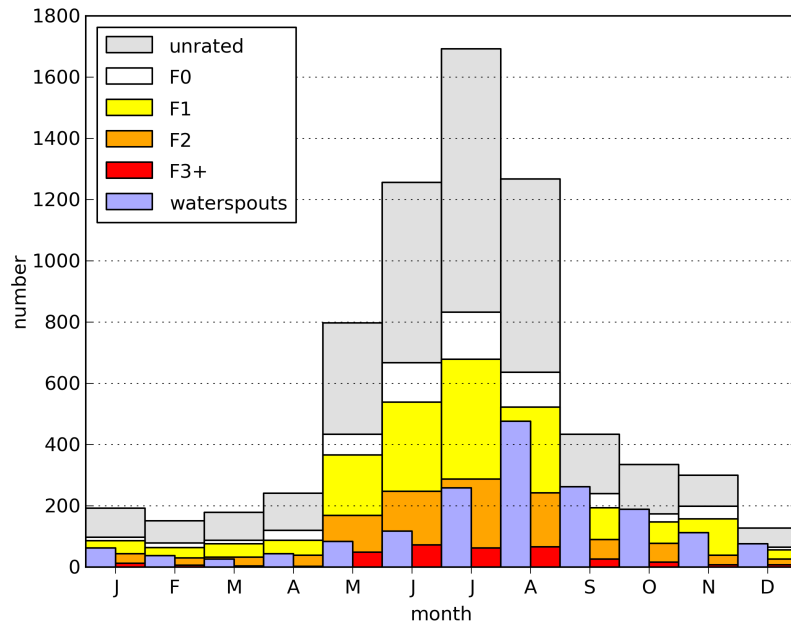
Figure 8: All tornadoes from the ESWD listed by the month they occurred in (Groenemeijer and Kühne (2014)).
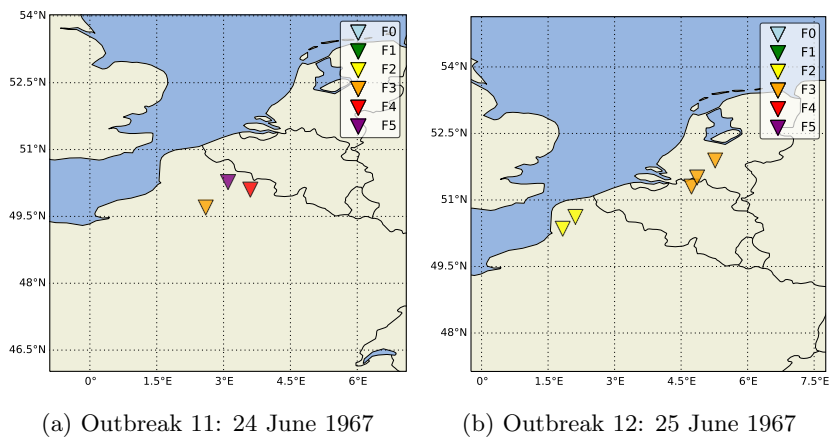

(a) Outbreak 11: 24 June 1967

(b) Outbreak 12: 25 June 1967

Figure 9: All tornadoes

DATE & TIME	F SCALE	PLACE	COUNTRY
1967-06-24 16:40:00	3	Davenescourt	FR
1967-06-24 17:35:00	5	Palluel	FR
1967-06-24 18:00:00	4	Pommereuil	FR
1967-06-25 09:45:00	2	Argoules	FR
1967-06-25 12:00:00	2	Merck-Saint-Liévin	FR
1967-06-25 14:15:00	3	Oostmalle	BE
1967-06-25 14:34:00	3	Ulicoten, Chaam, Gilze	NL
1967-06-25 15:15:00	3	Nieuwaal, Crob, Deil, Tricht, [W of] Buren	NL

Table 4: A table showing all tornadoes in outbreak 11 and 12.

are only available in regional languages and very little international research has been done. A record by Wessels (1968) gives insight in the synoptic setting of these outbreaks, as well as track and damage from the two tornadoes and accompanying severe weather occurring in The Netherlands on 25 June. Thanks to this record it was know that the synoptic setting for these tornado outbreaks featured a deep through over the Atlantic ocean and a high pressure ridge over central Europe, giving rise to a strong SSW flow over large parts of Western Europe. A setting like this is often termed a "Spanish Plume" and is the main setup for severe weather outbreaks in Western Europe (Delden (2001)). This particular setup of synoptic through and ridge maintained itself for three days (23rd to 25th) and gave rise to severe weather in France, The Benelux countries and western Germany. The first outbreak occurred on the 24th of June, where three tornadoes occurred in northern France. One of these tornadoes was given the exceptional rating of F5, which destroyed the town of Palluel. The two other tornadoes rated F4 and F3. These tornadoes can be seen in figure 9a. The next day, a similar synoptic pattern produced 5 more tornadoes: two again in northern France (both F2), one in northern Belgium (F3) and two in the Netherlands (both F3). These tornadoes can be seen in figure 9b. Unfortunately, both reanalysis sets here are not available for these times, so these outbreaks are not featured in the comparison.

4.1.2 Outbreak 17: 23 November 1981

This outbreak on 23 November 1981 in the UK features 104 tornado reports and an F scale sum of 74, making it by far the largest outbreak of all the outbreaks. With only 3 tornadoes of F2 strength (the rest being F1 or F0) it is not a particularly strong outbreak but the sheer amount of tornadoes makes this exceptional. On this day the cold front associated with a deep depression north-west of Scotland tracked across the UK from north-west to south-east. The cold front entered Scotland around 00 UTC and left south-east England around 18 UTC. The first reported tornado that day was at Amlwch in north-western Wales at 10:19 UTC and the last tornadoes were reported in West Mersea and Clacton-On-Sea at 15:45 UTC. meanwhile numerous tornadoes had occurred. Eyewitnesses of the tornadoes reported very dark skies and a loud roar accompanying the tornado. The times of the reported tornadoes matches the passage time of the cold front in Wales and western England, but in eastern
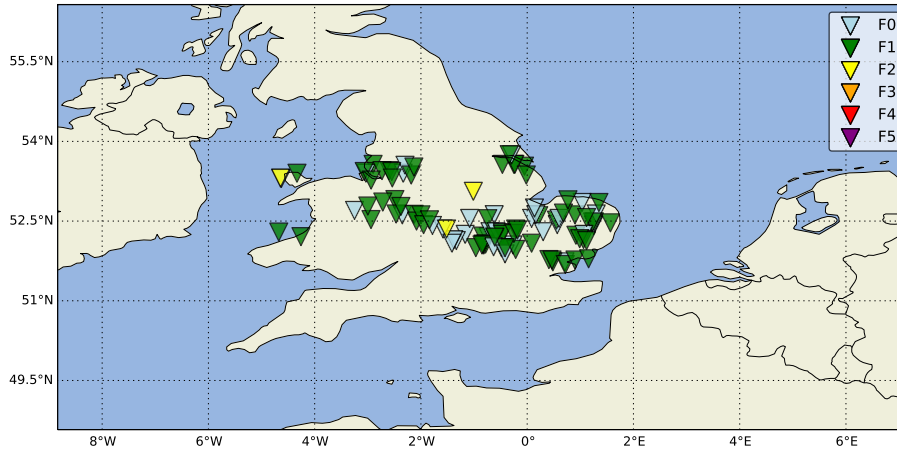
Figure 10: Outbreak 17: 23 November 1981

	F_SCALE	PLACE	COUNTRY
1981-11-23 10:19:00	1	Amlwch	UK
1981-11-23 10:34:00	0	Holyhead	UK
1981-11-23 10:34:00	2	Holyhead	UK
1981-11-23 10:45:00	1	Penrhos Feilw	UK
1981-11-23 11:00:00	1	Llanddaniel Fab	UK
1981-11-23 15:30:00	1	Coddenham	UK
1981-11-23 15:35:00	1	Mundon	UK
1981-11-23 15:40:00	1	Wymondham	UK
1981-11-23 15:45:00	1	West Mersea	UK
1981-11-23 15:45:00	1	Clacton-on-Sea	UK

Table 5: A table showing the first five and last five tornadoes of outbreak 17.

England reported tornadoes seemed to occur earlier than frontal passage. This suggests that the tornadoes in eastern England are perhaps associated with a pre-frontal convective line (Rowe and Meaden (1985)).

The high number of tornado reports were partly attributed to this outbreak being thoroughly researched. This was due to television and radio appeals. A large number reports would have gone unnoticed without these appeals (Rowe and Meaden (1985)). It is also likely that multiple tornado reports refer to the same tornado. This is great in terms of tornado reporting but since the amount of tornadoes is so large compared to the total amount of tornadoes in all outbreaks this outbreak cannot be used for comparisons of outbreak versus non-outbreak tornadoes. Therefore this outbreak will not be counted in those statistics. When comparing average values this is not an issue so there the outbreak will be included.
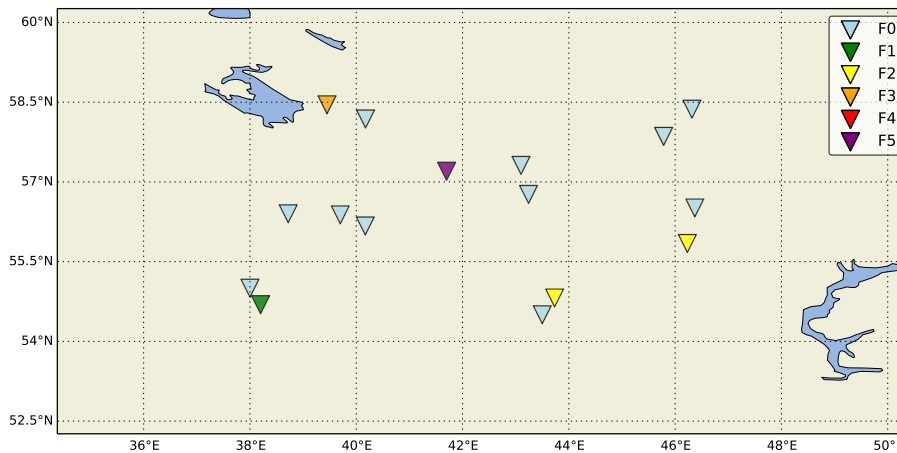
4.1.3   Outbreak 19: 9 June 1984

Figure 11: Outbreak 19: 9 June 1984

Outbreak 19 happened on 9 June 1984 in western Russia and consists of 17 tornadoes in total. About a large number of these tornadoes very little information is known which is why these tornadoes do not count towards the outbreak f scale sum since they are rated F0. The F scale criterium is met however due to a few strong tornadoes one of which has a rating of F5 near the city of Ivanovo. Next to producing 17 tornadoes, this severe weather outbreak also produced extremely large hail, making it one of the most severe in Russian history. A death toll of 400 has been cited with the F5 Ivanovo tornado (Finch and Bikos (2012)) but other sources cite different numbers (69, Groenemeijer and Kühne (2014)) so the exact number of deaths remain unknown. However, it stands clear that this outbreak was unusually strong.

It was shown by Finch and Bikos (2012) that this outbreak and especially the Ivanovo tornado was associated with high values of CAPE, shear and storm relative helicity.

	F_SCALE	PLACE	COUNTRY
1984-06-09 09:00:00	2	Alatyr'	RU
1984-06-09 09:00:00	2	Kanash	RU
1984-06-09 09:09:00	1	Sheremet'yevo	RU
1984-06-09 10:00:00	0	[unknown]	RU
1984-06-09 10:00:00	0	[unknown]	RU
1984-06-09 11:00:00	0	[unknown]	RU
1984-06-09 11:00:00	0	Danilov	RU
1984-06-09 11:30:00	0	Volosovo	RU
1984-06-09 12:00:00	0	Ponazyrevo	RU
1984-06-09 12:00:00	0	Chkalovsk	RU
1984-06-09 12:00:00	3	Golubkovo	RU
1984-06-09 12:00:00	0	Vetluga	RU
1984-06-09 12:05:00	5	Ivanovo	RU
1984-06-09 13:00:00	0	Yurevets	RU
1984-06-09 13:00:00	0	Luch	RU
1984-06-09 13:00:00	0	Vochmy	RU
1984-06-09 13:00:00	0	Shary	RU

Table 6: A table showing the tornadoes in outbreak 19.

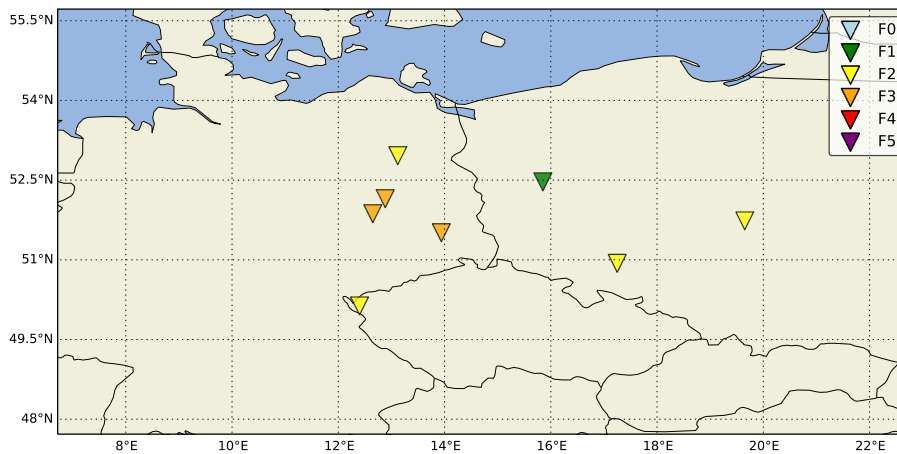### 4.1.4   Outbreak 27: 18 January 2007

Figure 12: Outbreak 27: 18 January 2007

The outbreak taking place at 18 January 2007 is part of the Kyrill windstorm that hit a large part of Europe on the same day. Large areas of heavy damage were delivered by non convective gusts by the windstorm. In addition to that, 8 tornadoes were part of an outbreak that day. Four of the tornadoes formed over eastern Germany with three of them having F3 status (the other one F2). One tornado occurred over the Ore Mountains on the border of Germany and the Czech Republic (F2). The other three occurred over Poland (2 F2 and 1 F1). Tornadoes occurring with windstorms are not a rare occurrence in Europe

24

	F_SCALE	PLACE	COUNTRY
2007-01-18 17:00:00	3	Brachwitz	DE
2007-01-18 17:30:00	2	Meseberg, Osterne	DE
2007-01-18 17:40:00	3	Lutherstadt Wittenberg	DE
2007-01-18 18:00:00	1	Silna	PL
2007-01-18 18:30:00	3	Lauchhammer	DE
2007-01-18 20:00:00	2	Gaj Olawski, Osiek, Chwalibozyce	PL
2007-01-18 22:00:00	2	Andrespol	PL
2007-01-18 22:19:00	2	Treben	CZ

Table 7: A table showing the tornadoes in outbreak 27.

in the winter. However normally these tornadoes are quite weak. The strength of these tornadoes was unprecedented during wintertime.

A case study presented by Gatzen et al. (2007) showed that ahead of the cold front that was associated with Kyrill, a number of storms formed within a well-mixed boundary layer in the warm sector ahead of the approaching cold front. These storms subsequently spawned the tornadoes in eastern Germany. The cause of the tornadoes in Poland has not been researched.

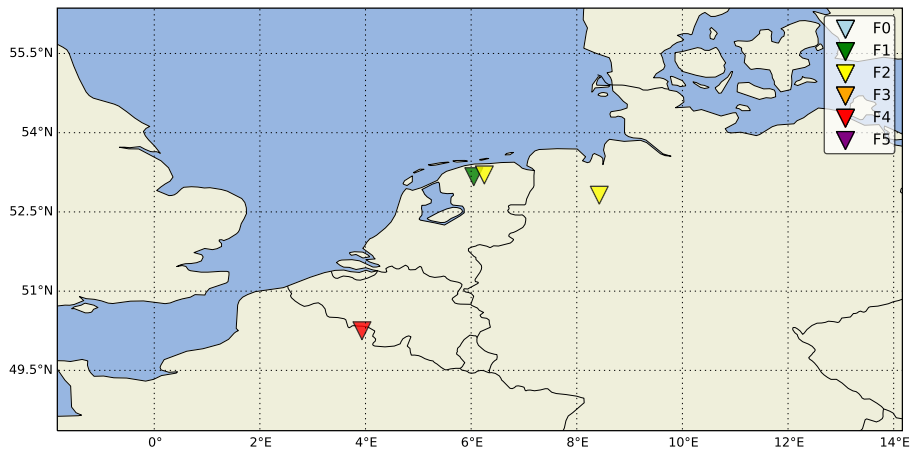### 4.1.5 Outbreak 31: 3 August 2008

Figure 13: Outbreak 31: 3 August 2008

This outbreak on the third of August 2008 features one F1, two F2 and one F4 tornado. Especially because of this F4 tornado near the town of Hautmont in northern France, this outbreak is well studied. The synoptic setting was characterized by a strong but shallow trough over the UK, which induced a jet streak over northern France and the Benelux countries. The jet streak was also accompanied by a strong low level jet which led to high low level wind shear values over the mentioned area. A reconstruction of the parameters prior to

	F_SCALE	PLACE	COUNTRY
2008-08-03 17:45:00	1	Oostermeer	NL
2008-08-03 18:45:00	2	Doezum, Lutjegast, Sebaldeburen	NL
2008-08-03 20:15:00	2	Altona	DE
2008-08-03 20:35:00	4	Hautmont	FR

Table 8: A table showing the tornadoes in outbreak 31.

the Hautmont Tornado by Wesolek and Mahieu (2011) showed that the 0-1 km Storm Relative Helicity was 519 m^2/s^2 and the 0-3 km Storm Relative Helicity was 564 m^2/s^2. These values generally indicate a high chance of tornadoes in storms that occur in these environments (Esterheld and Giuliano (2008)). These high values were not reproduced by CFSR nor by ERA-Interim for this outbreak.

4.2 Tornado Outbreaks and Reanalysis

In this section the results of the coupling of tornadoes and outbreaks to reanalysis data is explored. Since the tornadoes are now coupled to reanalysis data it is interesting to look at the results. In figure 14 the first of these images is plotted. In the figure $w_{max}(= \sqrt{2 * MLCAPE})$ is given for tornadoes outside outbreaks (grey), tornadoes outside outbreaks with F2 rating or higher (yellow), tornadoes in outbreaks (red) and outbreak averages (purple/yellow dots). As noted before the UK 1981 outbreak is too large in number and would skew the statistics of the individual tornadoes in the tornado outbreaks so it is not included in this statistic.
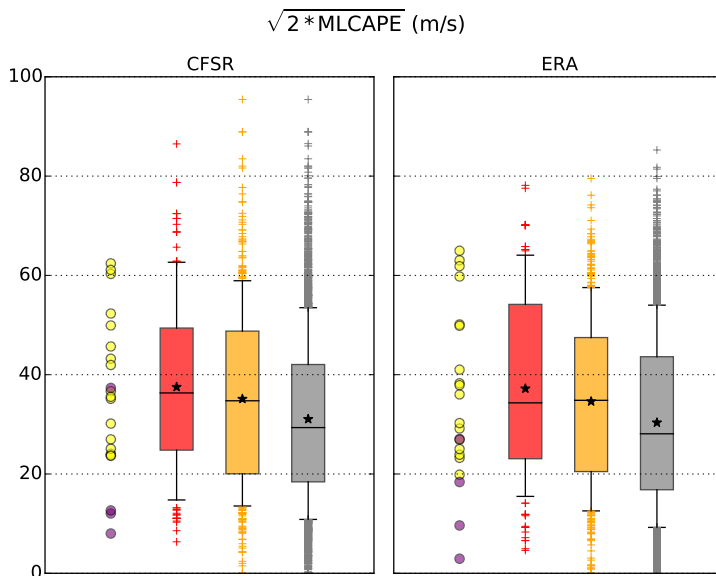

Figure 14: Boxplots showing $w_{max}(= \sqrt{2 * MLCAPE})$ for various distributions. Grey boxplot: Tornadoes outside outbreaks. Yellow boxplot: Tornadoes outside outbreaks of strength F2 and higher. Red boxplot: Outbreak tornadoes. Purple dots: Outbreak averages (winter). Yellow dots: Outbreak averages (summer). The boxes indicate the distribution between the first quartile (25%) and the third quartile (75%). The whiskers indicate the 10th percentile and the 90th percentile. The 50th percentile is indicated by the horizontal bar in the box and the average is indicated by the star. Tornadoes outside the whiskers are indicated by the pluses. On the left the values from CFSR are plotted and on the right the values from ERA-Interim.

It can be seen that the tornado outbreaks occur for a large range of MLCAPE. w_{max} for the tornadoes in outbreaks ranges from approximately 5 m/s to about 80 m/s (for CFSR almost up to 90 m/s). The non-outbreak tornadoes have even greater range because of the larger sample size. The figure also shows that outbreaks are characterized by slightly higher w_{max} compared to non-outbreak tornadoes. The values for outbreak tornadoes are slightly higher than for significant (F2+) non-outbreak tornadoes. This indicates that outbreaks are more

likely to occur with higher w_{max}. The tornado outbreak averages are divided between the summer half year (May - Oct) and the winter half year (Nov - Apr). Wintertime outbreaks are associated with lower w_{max} than summertime outbreaks. The differences between outbreak and non-outbreak tornadoes is visible in both reanalysis datasets. Although CFSR has more extreme values for both outbreaks and non-outbreak tornadoes, it also has more concentrated values around the median of the distributions. This is also illustrated by the fact that the outbreak averages are more spread out in the ERA-Interim data. However if one looks at all the factors then the CFSR and ERA-Interim data matches well for MLCAPE.
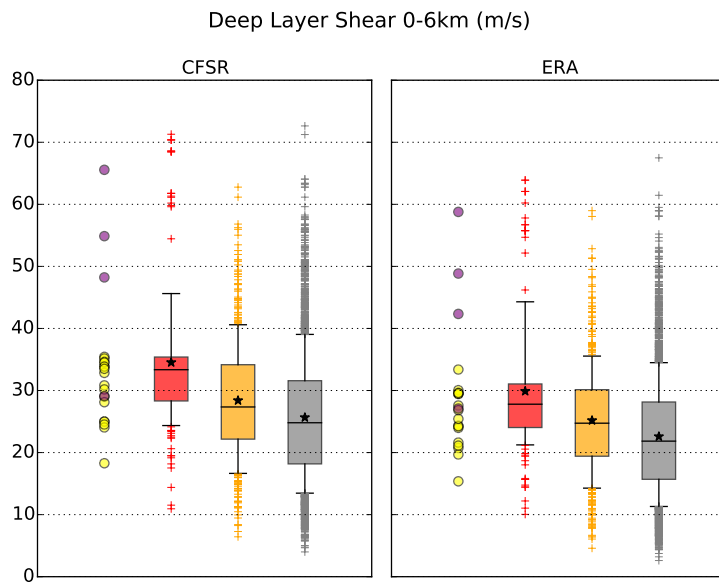

Figure 15: Boxplots showing DLS for various distributions. Grey boxplot: Tornadoes outside outbreaks. Yellow boxplot: Tornadoes outside outbreaks of strength F2 and higher. Red boxplot: Outbreak tornadoes. Purple dots: Outbreak averages (winter). Yellow dots: Outbreak averages (summer). The boxes indicate the distribution between the first quartile (25%) and the third quartile (75%). The whiskers indicate the 10th percentile and the 90th percentile. The 50th percentile is indicated by the horizontal bar in the box and the average is indicated by the star. Tornadoes outside the whiskers are indicated by the pluses. On the left the values from CFSR are plotted and on the right the values from ERA-Interim.

In figure 15 the same statistics are shown for the deep layer shear. It seems that tornado outbreaks generally favor high deep layer shear starting at 15 m/s for outbreaks averages. This is particularly true for the wintertime outbreaks, which are characterized by DLS values over 40 m/s. These values are higher than summertime outbreak values.

The summertime outbreaks DLS lie between 15 m/s and 35 m/s, whereas the

wintertime outbreaks range between 25 m/s and 65 m/s. Thus wintertime outbreaks are associated with higher shear than summer outbreaks.

A strong difference can be seen between non-outbreak tornadoes and outbreaks. The tornadoes in outbreaks are characterized by significantly higher values than non-outbreak tornadoes. This is seen in both CFSR and ERA-Interim. The outbreak tornadoes have on average even higher values compared to strong non-outbreak tornadoes. It can be seen that almost all outbreak averages are linked to higher DLS values than most non-outbreak tornadoes. This is a signal that tornado outbreaks as opposed to single events are more likely when DLS is very high.

One should also note the differences between the reanalysis sets. DLS in CFSR is notably higher than in ERA-Interim for all categories. Also in individual tornado cases CFSR has higher DLS than ERA-Interim (not shown).
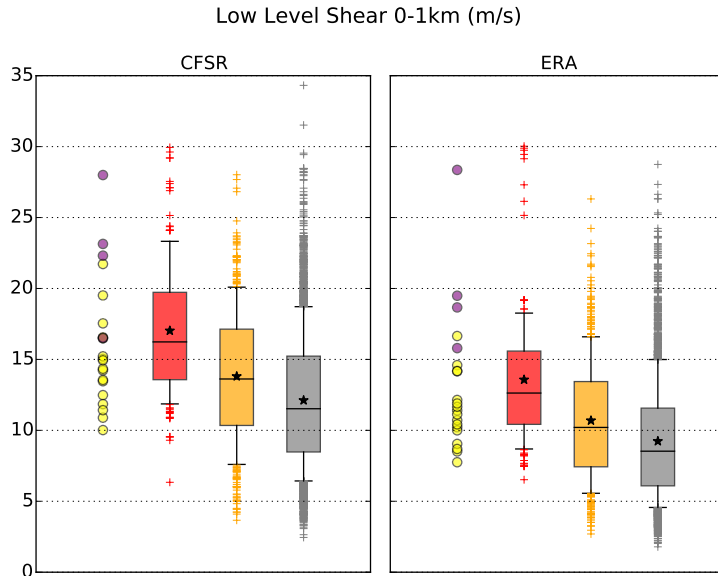

Figure 16: Boxplots showing LLS for various distributions. Grey boxplot: Tornadoes outside outbreaks. Yellow boxplot: Tornadoes outside outbreaks of strength F2 and higher. Red boxplot: Outbreak tornadoes. Purple dots: Outbreak averages (winter). Yellow dots: Outbreak averages (summer). The boxes indicate the distribution between the first quartile (25%) and the third quartile (75%). The whiskers indicate the 10th percentile and the 90th percentile. The 50th percentile is indicated by the horizontal bar in the box and the average is indicated by the star. Tornadoes outside the whiskers are indicated by the pluses. On the left the values from CFSR are plotted and on the right the values from ERA-Interim.

In figure 16 one can see a similar figure drawn for the low level shear. According to the data, tornado outbreaks generally favor high low level shear. CFSR has

tornado outbreak averages between 10 and 27.5 m/s, whereas ERA-Interim has values ranging between 7.5 and 27.5 m/s. As for DLS, wintertime outbreaks are associated with higher LLS than summertime outbreaks. The most important feature here is that tornado outbreaks are associated with much stronger shear than non-outbreak tornadoes. The differences between the two can be seen quite clearly in both CFSR and ERA-Interim. The values of tornado outbreaks are even significantly higher when compared to F2+ non-outbreak tornadoes. This seems to indicate that low level shear is a good discriminator between tornado outbreaks and individual tornadoes. However there is no threshold value as the distributions still overlap quite a bit. Also significant here are the differences between the reanalysis sets. Once more, CFSR seems to produce higher values of shear compared to ERA-Interim. This is true for all distributions shown here.
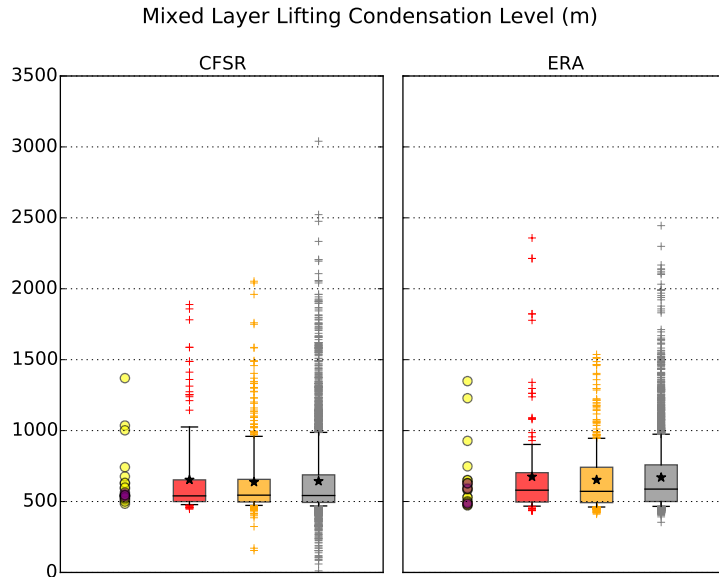

Figure 17: Boxplots showing MLLCL for various distributions. Grey boxplot: Tornadoes outside outbreaks. Yellow boxplot: Tornadoes outside outbreaks of strength F2 and higher. Red boxplot: Outbreak tornadoes. Purple dots: Outbreak averages (winter). Yellow dots: Outbreak averages (summer). The boxes indicate the distribution between the first quartile (25%) and the third quartile (75%). The whiskers indicate the 10th percentile and the 90th percentile. The 50th percentile is indicated by the horizontal bar in the box and the average is indicated by the star. Tornadoes outside the whiskers are indicated by the pluses. On the left the values from CFSR are plotted and on the right the values from ERA-Interim.

In figure 17, the same figure is plotted for MLLCL. Contrary to the previous figures very few differences can be seen in this figure. Tornado outbreaks and non-outbreak tornadoes have similar distributions. Most distributions have typically 90th percentile values lower than 1000 m. Summertime outbreaks are associated with slightly higher MLLCL than wintertime outbreaks. The high-

est values from tornadoes in tornado outbreaks can be found in ERA-Interim and the highest values from non-outbreak tornadoes are found in CFSR, but the differences between the two reanalysis sets are minor. Therefore there is no difference between outbreaks and single tornadoes in terms of MLLCL. All distributions have their highest density around 600-700 m. In CFSR a number of non-outbreak tornadoes have values under 400 m. This is attributed to corruption of the source data files in the download process. This is valid for a very small part of the distribution ($< 0.1\%$) and affects the boxplot very little.

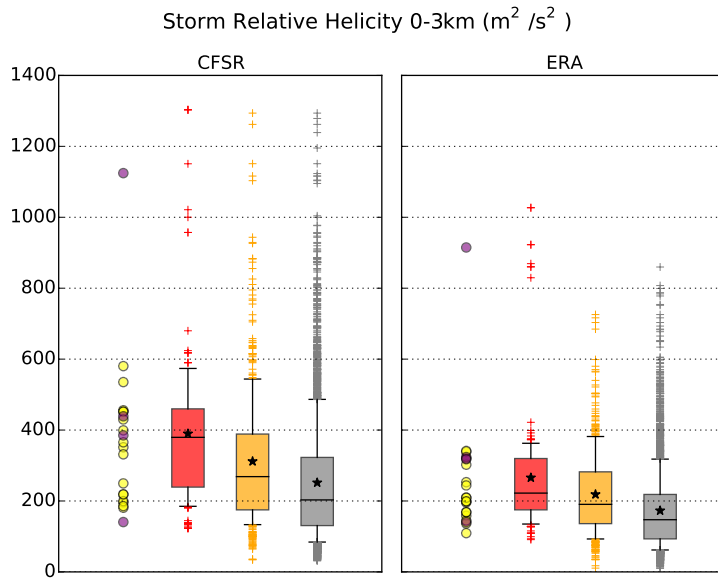Storm Relative Helicity 0-3km (m^2 /s^2)

Figure 18: Boxplots showing SRH 0-3 km for various distributions. Grey boxplot: Tornadoes outside outbreaks. Yellow boxplot: Tornadoes outside outbreaks of strength F2 and higher. Red boxplot: Outbreak tornadoes. Purple dots: Outbreak averages (winter). Yellow dots: Outbreak averages (summer). The boxes indicate the distribution between the first quartile (25%) and the third quartile (75%). The whiskers indicate the 10th percentile and the 90th percentile. The 50th percentile is indicated by the horizontal bar in the box and the average is indicated by the star. Tornadoes outside the whiskers are indicated by the pluses. On the left the values from CFSR are plotted and on the right the values from ERA-Interim.

In figure 18 the same figure is displayed for the storm relative helicity between 0 and 3 kilometers. It seems that tornado outbreaks also favor higher SRH 0-3 km compared to non-outbreak tornadoes. This signal is visible in both CFSR and ERA-Interim, although the increased signal is less visible in ERA. SRH 0-3 km is much smaller in ERA-Interim compared to CFSR. This difference is seen in all distributions. The difference is quite big as can be seen from the high value tail of the distributions where the extreme values of CFSR are much bigger than those of ERA-Interim. This is something that has been noted before with the deep layer shear and low level shear which is logical since the

shear and storm relative helicity are related. For CFSR outbreak values between the 10th and 90th percentile are between 200 and 600 m^2/s^2, whereas non-outbreak tornadoes have a lower range of 100 and 500 m^2/s^2. In ERA respective ranges are much lower with 150-350 m^2/s^2 for outbreaks and 100-300 m^2/s^2 for non-outbreak tornadoes. One outbreak in particular stands out from the other outbreaks as the values are much higher than the others. This is the Kyrill windstorm outbreak in January 2007 which was discussed before. This outbreak was characterized by extreme values of SRH 0-3 km in both CFSR and ERA-Interim. Though this outbreak has very high values, not all winter outbreaks have these high values. The others are comparable to the summer outbreaks. This is different from the shear values as those did show a higher shear with winter outbreaks.
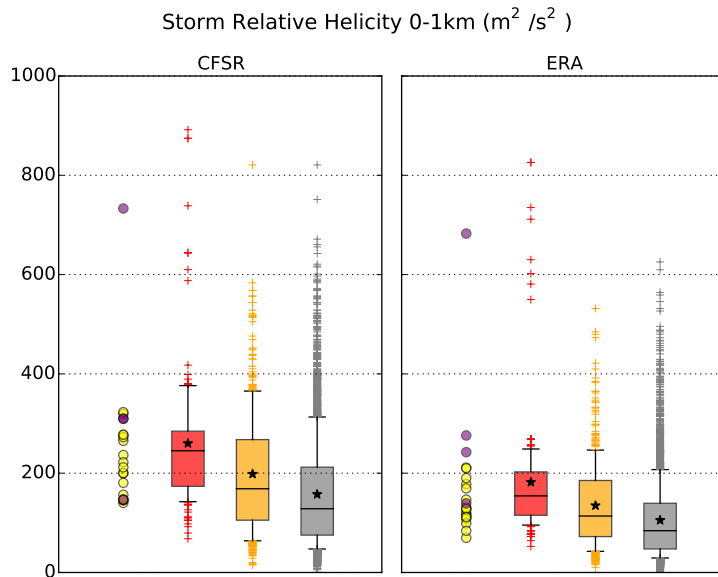

Figure 19: Boxplots showing SRH 0-1 km for various distributions. Grey boxplot: Tornadoes outside outbreaks. Yellow boxplot: Tornadoes outside outbreaks of strength F2 and higher. Red boxplot: Outbreak tornadoes. Purple dots: Outbreak averages (winter). Yellow dots: Outbreak averages (summer). The boxes indicate the distribution between the first quartile (25%) and the third quartile (75%). The whiskers indicate the 10th percentile and the 90th percentile. The 50th percentile is indicated by the horizontal bar in the box and the average is indicated by the star. Tornadoes outside the whiskers are indicated by the pluses. On the left the values from CFSR are plotted and on the right the values from ERA-Interim.

The figure for the storm relative helicity 0-1 km is very similar to that of the storm relative helicity 0-3 km. It can be seen that outbreaks have again higher values when compared to non-outbreak tornadoes. For CFSR outbreak between the 10th and 90th percentile are characterized by values between 150 and 350 m^2/s^2, whereas non-outbreak tornadoes have a lower range of 50 and 300 m^2/s^2.

In ERA, the respective ranges are much lower with 100-250 m^2/s^2 for outbreaks and 50-200 m^2/s^2 for non-outbreak tornadoes. Again, CFSR presents higher values when compared to ERA-Interim for all distributions. The Kyrill windstorm outbreak again stands out with much higher values than the rest of the outbreaks.

5   Conclusion

The European Severe Weather Database contains 5720 tornado reports between 1 Jan 1900 and 31 Aug 2014 in Europe. Tornado record frequency has been increasing tremendously during the last 15 years. Records are plentiful in countries in Western-, Central- and Eastern Europe, but more scarce in Northern and Southern Europe. Despite these shortcomings in the tornado data, a tornado outbreak list has been created using a tornado outbreak definition based on the temporal and spacial distance between tornado report in the ESWD. The values r and t, which denote respectively the spatial and temporal distance that is allowed between two tornado reports to join these tornadoes together in a group, are set to 500 km and 6 hours. Additionally a requisite has been set for these tornado groups to be tornado outbreaks. This requirement is the sum of the F scale values of the tornadoes in the tornado groups. This sum of the F scale value is set to 7. The values for t, r and the F scale sum yield 36 tornado outbreaks in the period 1 Jan 1900 - 31 Aug 2014. Among these outbreaks are some of Europe's most severe tornado events. Examples are the strong tornado outbreaks in northern France and the Benelux on the 24 and 25 June 1967, the large tornado outbreak in Russia on 9 June 1984 and more recently the strong wintertime tornado outbreak in Germany and Poland on 18 January 2007. The list of identified outbreaks includes several "well-known" events in the sense that they were subject of prior scientific research. Therefore this technique is a valid technique of defining tornado outbreaks in Europe. Some variation can still by applied by varying the values of r and t or by choosing a different selection for outbreaks. For example instead of using the sum of the F scale values one can select by number of tornadoes or minimal F strength. This way a different list will be created but it will still have some similarities to the current list, implying that the stronger and/or bigger outbreaks will still be included.

By using two reanalysis datasets and computing convective parameters from these datasets, tornado reports have been linked to atmospheric variables at the time of the tornado. The convective parameters that have been computed are: mixed layer convective available potential energy (MLCAPE), deep layer shear (DLS), low level shear (LLS), mixed layer lifting condensation level (MLLCL) and the storm relative helicity (SRH) in the layers 0-3 km and 0-1 km. Due to the discrete nature of the reanalysis data there is a need to assign values to the time and location of the tornado. Values have been selected from a 3 x 3 degree box surrounding the tornado. For all values the maximum value from this 3 x 3 degree box has been taken except lifting condensation level for which the minimum value is instead selected. These assigned values have been analyzed in boxplots where tornado outbreak values were compared to non-outbreak tornadoes. From the figures it can be derived that the values of MLCAPE, DLS, LLS and SRH (both 0-3 km and 0-1 km) are generally higher in the case of tornado outbreaks when compared to non-outbreak tornadoes. Of these parameters the LLS showed the biggest difference. Even when compared to significant (F2+) non-outbreak tornadoes the tornado outbreaks were still characterized by higher values. The parameter MLLCL did not show any differences between the analyzed distributions.

Wintertime (Nov-Apr) tornado outbreaks are characterized by higher DLS and

LLS and lower MLCAPE compared to summertime (May-Oct) tornado outbreaks.

Significant differences between the ERA-Interim and CFSR datasets have been found. For the parameters DLS, LLS and SRH (0-3 km and 0-1 km) CFSR assigned values are higher than ERA-Interim. Especially for these parameters CFSR showed much higher percentile values compared to ERA-Interim. For the parameter MLLCL and MLCAPE no significant differences were found.

6 Discussion

Tornado data in the ESWD varies a lot in space and time: Some countries have better coverage than others and tornado records have been increasing in recent years. But even in the best covered countries it is possible that tornadoes are not reported. For example, when a tornado does not hit anything. Therefore tornadoes may go unnoticed. Furthermore a large number of tornadoes are unrated. Most of them are likely to be F0-F1 but it is possible that some significant tornadoes are unrated. Thus the rating of tornadoes themselves might be uncertain or unreliable. These are all causes that influence the detection of tornado outbreaks. Therefore the 36 tornado outbreaks that are detected should not be taken as a tornado climatology for Europe, because there is too much uncertainty in the tornado reports.

The coupling of reanalysis data to tornadoes is constructed to be as representative as possible. However it is not the true value of that parameter at the time and place of the tornado. Due to the discrete nature of the reanalysis fields it is impossible to know the true value. The detection of maximum or minimum value in a "box" around the tornado may over- or underestimate the value, depending on the variable and situation.

The reanalysis datasets are an attempt to rebuild the state of the atmosphere in the past. However significant differences have been found between the calculated convective parameters from these two reanalysis datasets used in this study. This rises a lot of questions on how representative these datasets really are. Why do these datatsets differ so much? Does it only differ in specific cases or is it a constant bias? How different are these datasets compared to other reanalysis datasets? Further study should be done to find answers to these questions.

References

Bissolli, P. et al. (2007). "Tornadoes in Germany 1950–2003 and their relation to particular weather conditions". In: *Global and Planetary Change* 57.1, pp. 124–138.

Bluestein, H. B. (1999). "A history of severe-storm-intercept field programs". In: *Weather and forecasting* 14.4, pp. 558–577.

Bolton, D. (1980). "The computation of equivalent potential temperature". In: *Monthly weather review* 108.7, pp. 1046–1053.

Bunkers, M. J. et al. (2000). "Predicting supercell motion using a new hodograph technique". In: *Weather and forecasting* 15.1, pp. 61–79.

Bunkers, M. J. et al. (2002). "P8. 2 THE IMPORTANCE OF PARCEL CHOICE AND THE MEASURE OF VERTICAL WIND SHEAR IN EVALUATING THE CONVECTIVE ENVIRONMENT". In:

Davies, J. M. and Johns, R. H. (1993). "Some wind and instability parameters associated with strong and violent tornadoes: 1. Wind shear and helicity". In: *The Tornado: Its Structure, Dynamics, Prediction, and Hazards*, pp. 573–582.

Dee, D. et al. (2011). "The ERA-Interim reanalysis: Configuration and performance of the data assimilation system". In: *Quarterly Journal of the Royal Meteorological Society* 137.656, pp. 553–597.

Delden, A. van (2001). "The synoptic setting of thunderstorms in western Europe". In: *Atmospheric research* 56.1, pp. 89–110.

Doswell III, C. et al. (2006). "A simple and flexible method for ranking severe weather events". In: *Weather and forecasting* 21.6, pp. 939–951.

Dotzek, N. (2001). "Tornadoes in Germany". In: *Atmospheric research* 56.1, pp. 233–251.

Dotzek, N. (2003). "An updated estimate of tornado occurrence in Europe". In: *Atmospheric Research* 67, pp. 153–161.

Esterheld, J. M. and Giuliano, D. J. (2008). "Discriminating between tornadic and non-tornadic supercells: A new hodograph technique". In: *E-Journal of Severe Storms Meteorology* 3.2.

Finch, J. D. and Bikos, D. (2012). "Russian tornado outbreak of 9 June 1984". In: *E-Journal of Severe Storms Meteorology* 7.4.

Fujita, T. T. et al. (1971). *Proposed characterization of tornadoes and hurricanes by area and intensity*. University.

Galway, J. G. (1977). "Some climatological aspects of tornado outbreaks". In: *Monthly Weather Review* 105.4, pp. 477–484.

Gatzen, C. et al. (2007). "A CLOSE LOOK AT A SEVERE MESOSCALE CONVECTIVE SYSTEM DURING THE "KYRILL"-WINTER STORM OVER CENTRAL EUROPE". In: *4th European Conference on Severe Storms*.

Groenemeijer, P. and Kühne, T. (2014). "A climatology of tornadoes in Europe: Results from the European Severe Weather Database". In: *Monthly Weather Review* 142.12, pp. 4775–4790.

Grünwald, S. and Brooks, H. (2011). "Relationship between sounding derived parameters and the strength of tornadoes in Europe and the USA from reanalysis data". In: *Atmospheric Research* 100.4, pp. 479–488.

Pautz, M. E. (1969). *Severe local storm occurrences, 1955-1967*. US Department of Commerce, Environmental Science Services Administration, Weather Bureau.

Rowe, M. and Meaden, G. (1985). "Britain's greatest tornado outbreak". In: *Weather* 40.8, pp. 230–235.

Saha, S. et al. (2010). "The NCEP climate forecast system reanalysis". In: *Bulletin of the American Meteorological Society* 91.8, pp. 1015–1057.

Saha, S. et al. (2014). "The NCEP climate forecast system version 2". In: *Journal of Climate* 27.6, pp. 2185–2208.

Wegener, A. (1917). *Wind-und Wasserhosen in Europa*. Vol. 60. F. Vieweg & Sohn.

Weisman, M. L. and Klemp, J. B. (1982). "The dependence of numerically simulated convective storms on vertical wind shear and buoyancy". In: *Monthly Weather Review* 110.6, pp. 504–520.

Wesolek, E. and Mahieu, P. (2011). "The F4 tornado of August 3, 2008, in Northern France: Case study of a tornadic storm in a low CAPE environment". In: *Atmospheric Research* 100.4, pp. 649–656.

Wessels, H. (1968). "De zware windhozen van 25 juni 1967". In: *Hemel en Dampkring* 66, pp. 155–178.

Acknowledgements